Neurobiology of Disease

Brain-Wide Insulin Resistance, Tau Phosphorylation Changes, and Hippocampal Neprilysin and Amyloid-β Alterations in a Monkey Model of Type 1 Diabetes

Jose Morales-Corraliza,[1,2] Harrison Wong,[1] Matthew J. Mazzella,[1] Shaoli Che,[1,2] Sang Han Lee,[1] Eva Petkova,[1,3] Janice D. Wagner,[5] Scott E. Hemby,[6] Stephen D. Ginsberg,[1,2,4] and Paul M. Mathews[1,2]

[1]Nathan Kline Institute for Psychiatric Research, Orangeburg, New York 10962, Departments of [2]Psychiatry, [3]Child and Adolescent Psychiatry, and [4]Neuroscience and Physiology, New York University Langone Medical Center, New York, New York 10016, [5]Department of Pathology, Wake Forest School of Medicine, Winston-Salem, North Carolina 27157, and [6]Fred Wilson School of Pharmacy, High Point University, High Point, North Carolina 27268

Epidemiological findings suggest that diabetic individuals are at a greater risk for developing Alzheimer's disease (AD). To examine the mechanisms by which diabetes mellitus (DM) may contribute to AD pathology in humans, we examined brain tissue from streptozotocin-treated type 1 diabetic adult male vervet monkeys receiving twice-daily exogenous insulin injections for 8–20 weeks. We found greater inhibitory phosphorylation of insulin receptor substrate 1 in each brain region examined of the diabetic monkeys when compared with controls, consistent with a pattern of brain insulin resistance that is similar to that reported in the human AD brain. Additionally, a widespread increase in phosphorylated tau was seen, including brain areas vulnerable in AD, as well as relatively spared structures, such as the cerebellum. An increase in active ERK1/2 was also detected, consistent with DM leading to changes in tau-kinase activity broadly within the brain. In contrast to these widespread changes, we found an increase in soluble amyloid-β (Aβ) levels that was restricted to the temporal lobe, with the greatest increase seen in the hippocampus. Consistent with this localized Aβ increase, a hippocampus-restricted decrease in the protein and mRNA for the Aβ-degrading enzyme neprilysin (NEP) was found, whereas various Aβ-clearing and -degrading proteins were unchanged. Thus, we document multiple biochemical changes in the insulin-controlled DM monkey brain that can link DM with the risk of developing AD, including dysregulation of the insulin-signaling pathway, changes in tau phosphorylation, and a decrease in NEP expression in the hippocampus that is coupled with a localized increase in Aβ.

Key words: alzheimer's disease; diabetes; hippocampus; neprilysin; nonhuman primate; streptozotocin

---

Significance Statement

Given that diabetes mellitus (DM) appears to increase the risk of developing Alzheimer's disease (AD), understanding the mechanisms by which DM promotes AD is important. We report that DM in a nonhuman primate brain leads to changes in the levels or posttranslational processing of proteins central to AD pathobiology, including tau, amyloid-β (Aβ), and the Aβ-degrading protease neprilysin. Additional evidence from this model suggests that alterations in brain insulin signaling occurred that are reminiscent of insulin signaling pathway changes seen in human AD. Thus, in an *in vivo* model highly relevant to humans, we show multiple alterations in the brain resulting from DM that are mechanistically linked to AD risk.

Introduction

Diabetes mellitus (DM) puts patients at risk for multifactorial cognitive decline. For many decades, it has been understood that

DM-driven vascular disease can lead to stroke and subsequent cognitive compromise (McCrimmon et al., 2012). Moreover, epidemiological studies show a link between DM and an increased risk for Alzheimer's disease (AD) during aging (Akomolafe et al., 2006; Biessels et al., 2006; Sims-Robinson et al., 2010). In exper-

imental rodent models of DM, changes in tau protein phosphorylation are a consistent finding, suggesting that DM and DM-mediated insulin dysregulation may be linked to AD through a mechanism that involves DM promoting the accumulation of hyperphosphorylated tau, one of the pathological hallmarks of AD (for review, see El Khoury et al., 2014). Increases in brain tau phosphorylation have been reported in rodent models of both type 1 DM (Planel et al., 2007; Ke et al., 2009; Jolivalt et al., 2010; Papon et al., 2013) and type 2 DM (Li et al., 2012; Jung et al., 2013). In addition to tau pathology, AD is further characterized by the pathological accumulation of amyloid-β (Aβ) peptides. In rodent models, the effect of DM on Aβ is less clear. An increase in deposited human Aβ in total brain homogenate has been reported in the 5XFAD mouse model after treatment with the pancreatic β-cell destroying toxin streptozotocin (STZ) and without subsequent exogenous insulin support (Devi et al., 2012). In contrast, in a human amyloid-β precursor protein (APP) transgenic mouse model (APP23) crossed with the ob/ob model of DM, no overall increase in Aβ burden was detected, although more human Aβ was observed in brain microvessels (Takeda et al., 2010). Whereas the rodent tau findings have primarily examined the endogenously expressed tau protein (Planel et al., 2007; Jolivalt et al., 2010; Li et al., 2012; Jung et al., 2013; Papon et al., 2013), Aβ studies relied on models overexpressing APP containing AD-promoting mutations, which may not accurately reflect a DM effect on the metabolism of the endogenous APP. Moreover, APP has been suggested to modulate glucose and insulin homeostasis (Needham et al., 2008) and to worsen the diabetic phenotype in type 2 DM mouse models (Takeda et al., 2010), suggesting the potential for a interrelationship between APP expression and DM that may alter DM effects in an APP overexpression model.

Findings from human studies suggest that insulin signaling within the brain may play a central role in mediating cognitive and AD risk (Garcia-Casares et al., 2014; de la Monte and Tong, 2014; De Felice and Lourenco, 2015). In the AD brain, particularly within the hippocampus, molecular changes in the insulin-signaling pathway occur that resemble peripheral tissue insulin resistance. Talbot et al. (2012) have shown that inhibitory phosphorylation of brain insulin receptor substrate 1 (IRS1), a key player in cellular insulin signaling (Gual et al., 2005), increases during the progression from mild cognitive impairment (MCI) to AD in nondiabetic patients. Consistent with the idea that disruptions in brain insulin signaling occur in AD, exogenous intranasal insulin has been shown to improve cognition in MCI and early AD patients (Craft et al., 2012; Hölscher, 2014; Claxton et al., 2015) and reduce AD-like pathology in rodent models (Chen et al., 2014a,b). Therefore, intranasal insulin therapy is being evaluated as a potential cognitive enhancing intervention for MCI and AD (Rdzak and Abdelghany, 2014; Yarchoan and Arnold, 2014).

To characterize the pathways by which DM-driven changes in the brain may predispose an individual to AD, we have examined frozen brain tissue from a previously reported cohort of type 1 diabetic vervet monkeys (*Chlorocebus aethiops*) that were maintained for 8 – 20 weeks after STZ treatment with twice-daily insulin injections (Kavanagh et al., 2011; Saisho et al., 2011). In addition to examining IRS1 as a biochemical marker of changes in brain insulin signaling, tau, Aβ, and key proteins responsible for their processing were examined in multiple brain regions. Our findings in this nonhuman primate model of type 1 DM suggest that a brain-wide increase in tau phosphorylation coupled with an increase in Aβ localized to the hippocampus and temporal lobe are early events that would, over many years as an

individual ages, predispose the human diabetic brain to clinically relevant AD pathology.

Materials and Methods

Study approval. All experimental procedures involving animals in this study were approved by and complied with the guidelines of the Institutional Animal Care and Use Committee of Wake Forest University Health Sciences.

Monkeys. Adult male vervet monkeys (*Chlorocebus aethiops*), aged 6 – 8 years (mean, 6.9 ± 0.2 years), were used for this study (Kavanagh et al., 2011; Saisho et al., 2011). All animals were fed a standard monkey chow diet (PMI Nutrition International). Before treatment, monkeys were stratified into two matched groups (treatment cohort and control cohort) based on age, body weight, and glycemic control (Kavanagh et al., 2011). Fifteen monkeys were infused with STZ (Zanosar; 100 mg/ml in normal saline; SICOR Pharmaceuticals) at a dose of 45 or 55 mg/kg; 10 control monkeys were administered an equivalent volume of saline. Hyperglycemia was confirmed 2 d later in the STZ-treated monkeys after STZ doses (Kavanagh et al., 2011). Monkeys were then started on insulin therapy, receiving twice-daily insulin injections [70% intermediate-acting (neutral protamine Hagedorn), 30% short-acting (regular insulin), Novolin 70/30; Novo Nordisk]. At least twice weekly, insulin doses were adjusted as needed based on whole-blood glucose measurements determined via glucometer measured ~3 h after insulin dosing and feeding (postprandial) to avoid diabetic ketoacidosis. In this study, we determined blood glucose measurements from plasma collected via percutaneous femoral venipuncture from monkeys before any STZ or saline treatment, 1 week before the animals were killed, and at the time the animals were killed. Ongoing insulin therapy was withheld for 18 h before the blood sampling done 1 week in advance of when the animals were killed and then resumed. Additional clinical analyses of glycemic indices including additional blood plasma glucose measurements, insulin levels, hemoglobin A1c levels, and plasma lipid measurements have been reported previously (Kavanagh et al., 2011; Saisho et al., 2011). For Western blot, qPCR, and Aβ ELISA analyses from brain, we examined 17 monkeys killed at 4 weeks (n = 1 control; n = 0 diabetic), 8 weeks (n = 3 control; n = 3 diabetic), 12 weeks (n = 0 control; n = 1 diabetic), 16 weeks (n = 2 control; n = 4 diabetic), and 20 weeks (n = 1 control; n = 2 diabetic) after STZ or saline treatment. For plasma Aβ ELISA measurements, we analyzed a total of 25 samples, consisting of these 17 animals and an additional eight (n = 3 control; n = 5 diabetic; Kavanagh et al., 2011). These additional eight monkeys were treated identically to the previously described 17 monkeys, but brain tissue was not available. These monkeys were killed at 4 weeks (n = 1 control; n = 3 diabetic), 12 weeks (n = 1 control; n = 2 diabetic), and 20 weeks (n = 1 control; n = 0 diabetic) after STZ or saline treatment. Diabetic animals received insulin treatment on the day the animals were killed. All collected tissues and terminal blood plasmas were immediately snap-frozen for subsequent biochemical analyses; no tissue was fixed or stored frozen in a cryopreservant. Regional dissections of the hippocampus, frontal cortex, superior temporal cortex, and cerebellum were obtained from frozen coronal-sectioned brain slabs.

Antibodies. Full-length APP was detected with the antibody C1/6.1 (Mathews et al., 2002). Antibodies 22C11 (Millipore), JRF/Aβtot/17 (Morales-Corraliza et al., 2013), and 242 (Nishitomi et al., 2006) recognize soluble APP total (sAPP total: sAPPα + sAPPβ), sAPPα, and sAPPβ, respectively, APP metabolites that we have shown previously to be highly stable in the brain (Morales-Corraliza et al., 2009). Monoclonal antibody 56C6 (CD10; Novocastra) was used to detect neprilysin (NEP). Insulin-degrading enzyme (IDE) was recognized with the antibody IDE1 (Qiu et al., 1998; a gift from Dr. Dennis Selkoe, Ann Romney Center for Neurologic Diseases, Harvard Institutes of Medicine, Boston, MA). Endothelin Converting Enzyme 1 (ECE1) was detected with an antibody from Abgent. Levels of receptor for advanced glycation end products (RAGEs) and low-density lipoprotein receptor-related protein-1 (LRP1) were detected with the antibodies anti-RAGE (Abcam) and anti-LRP1 (American Diagnostica), respectively. Phosphorylated tau was detected using the antibodies PHF-1 (phospho-epitope at Ser396/404; a gift from
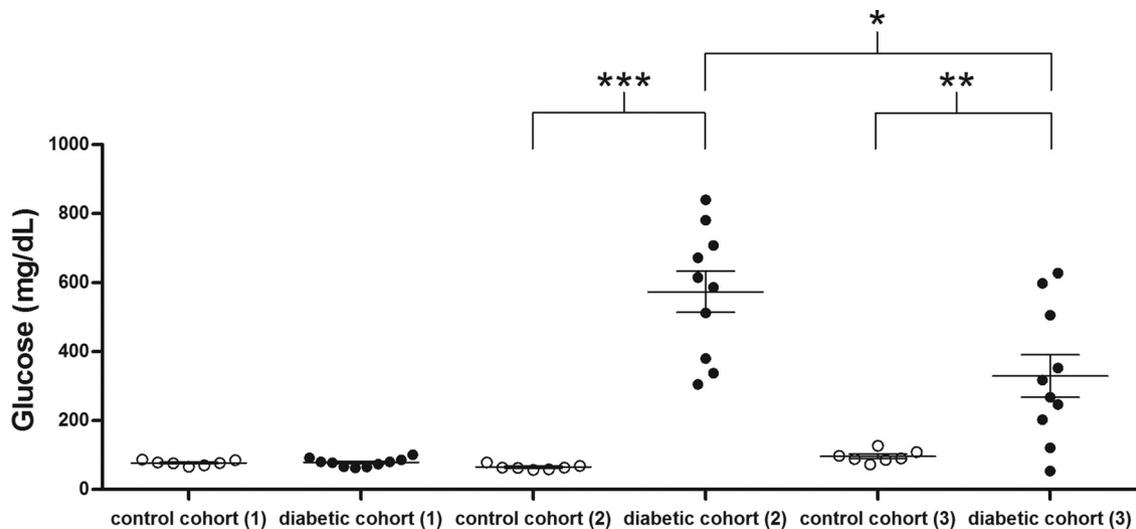
Figure 1. Hyperglycemia after STZ treatment. Baseline plasma glucose levels were determined from plasma obtained before STZ treatment (1; pretreatment), 1 week before the animals were killed and after withholding ongoing insulin therapy for 18 h (2; insulin treatment withheld), and obtained the day of the necropsy and after receiving standard insulin treatment (3; at necropsy), as well as from control animals at each of these points. Monkeys had food available *ad libitum* before a morning blood sampling. $*p < 0.05$; $**p < 0.01$; $***p < 0.001$.

Dr. Peter Davies, Feinstein Institute for Medical Research, Hofstra North Shore-LIJ School of Medicine, Manhasset, NY; Weaver et al., 2000) and CP13 (phospho-epitope at Ser202; a gift from Dr. Peter Davies). The tau1 antibody (Millipore) was used to recognize tau protein that is not phosphorylated at serines 195, 198, 199, and 202 (Szendrei et al., 1993), and DA9 (a gift from Dr. Peter Davies) detects total tau independent of its phosphorylation state. Tau kinases/phosphatases extracellular signal-regulated protein kinases 1 and 2 (ERK1/2), phospho-ERK1/2 (Thr202/204), glycogen synthase kinase-3β (GSK3β), phospho-GSK3β (Ser9), and protein phosphatase PP2A and PP2B were detected with antibodies from Cell Signaling Technology and p35/p25 and cyclin-dependent kinase 5 (CDK5) were from Santa Cruz Biotechnology. ERK1/2-mediated phosphorylation of tau at both the PHF-1 and CP13 antibody epitope sites has been described previously (Reynolds et al., 2000). Phosphorylated IRS1 was detected using an antibody that recognizes the phospho-epitope at Ser616 (Thermo Fisher Scientific; human protein amino acid numbering), whereas total IRS1 levels were detected with an antibody from Cell Signaling Technology.

Brain processing, Western blot analysis, and ELISA measurements. Ten percent (weight/volume) homogenates were prepared from regionally dissected frozen gray matter for biochemical analyses (Schmidt et al., 2012a). An aliquot of the homogenates was extracted in diethylamine for Aβ sandwich ELISA (Schmidt et al., 2012b) and for sAPP isolation before Western blot analyses as described previously (Morales-Corraliza et al., 2009). For Western blot analysis, brain proteins were sized by SDS-PAGE, transferred to polyvinylidene difluoride membrane, and incubated with antibodies as described previously (Morales-Corraliza et al., 2009).

Liver and plasma samples. Western blot analysis of hepatic tissue (using homogenates prepared as for brain samples) and blood plasma samples to detect secreted forms of LRP1 (Sagare et al., 2007), RAGE (Yan et al., 2000), NEP (Soleilhac et al., 1996), and IDE (Qiu et al., 1998) were performed using the antibodies described above. ECE1 was not detected in blood plasma. Aβ in blood plasma was detected by sandwich ELISA as described above for brain samples.

qPCR. qPCR was performed in triplicate on frozen tissue samples dissected from the hippocampus, temporal cortex, frontal cortex, and cerebellum of STZ-treated and control monkeys. Samples were assayed on a qPCR cycler (7900HT; Applied Biosystems). TaqMan hydrolysis probes designed for NEP (Hs01115448_m1), IDE (Hs00610452_m1), and glyceraldehyde-3 phosphate dehydrogenase (GAPDH; Rh02621745_g1) were used as described previously (Ginsberg et al., 2010; Alldred et al., 2012). Standard curves and cycle threshold (Ct) were generated using standards obtained from total monkey brain RNA. The ddCT method was used to determine relative gene level differences, and data are presented as an expression level percent of saline-treated controls as described previously (Alldred et al., 2009). A negative control consisted of the reaction mixture assayed without input RNA.

Statistical analysis. Data analysis in this study includes animals killed at all time points after STZ or saline treatment. Analyses of individual time points after STZ treatment were precluded by the low sample size per time point. An analysis (data not shown) indicated a negligible time effect on difference between groups in phospho-tau, Aβ, and NEP measurements. For this analysis, time effect was assessed in a way that tested group difference after removing subjects sequentially in time. Western blots were quantitated using NIH ImageJ (http://rsb.info.nih.gov). The nonparametric Wilcoxon's test was used to compare diabetic and control findings using the program "PROC NPAR1WAY" with exact p values in SAS 9.4 (Proc Mixed in SAS software; SAS Institute). This approach generated p values from the empirical distribution by enumerating samples (Agresti, 2007). Data were plotted on GraphPad Prism (GraphPad Software) for graphical output. β-Tubulin expression was used as a control for multiple testing in the analysis of Western blot data. Throughout, results are expressed as the mean ± SEM; nonsignificant findings have a p value >0.05, whereas statistically significant findings are indicated as shown: $*p < 0.05$, $**p < 0.01$, and $***p < 0.001$.

Results

Kavanagh et al. (2011) have demonstrated that administration of STZ (45 or 55 mg/kg) in vervet monkeys resulted in a dramatic reduction in endogenous insulin levels and hyperglycemia. Frozen brain tissue, blood plasma, and liver tissue were obtained from this monkey model of type 1 DM for this study. Control animals that were treated with saline and animals treated with STZ had similar baseline plasma glucose concentrations (Fig. 1, (1); pretreatment); 78 ± 4 mg glucose/dl in the diabetic monkey cohort before STZ treatment vs 77 ± 3 mg/dl in control monkeys before saline treatment; $p > 0.05$; additional glycemic index markers were given by Kavanagh et al., 2011). Two days after STZ treatment and the onset of hyperglycemia, twice-daily insulin therapy was initiated as detailed previously to prevent diabetic ketoacidosis (Kavanagh et al., 2011; see also Materials and Methods). A profound loss of pancreatic β-cells was shown to persist over the period that these animals were maintained (8–20 weeks) after STZ treatment (Saisho et al., 2011). To confirm a persistent diabetic state in these animals, 1 week before necropsy, the STZ-
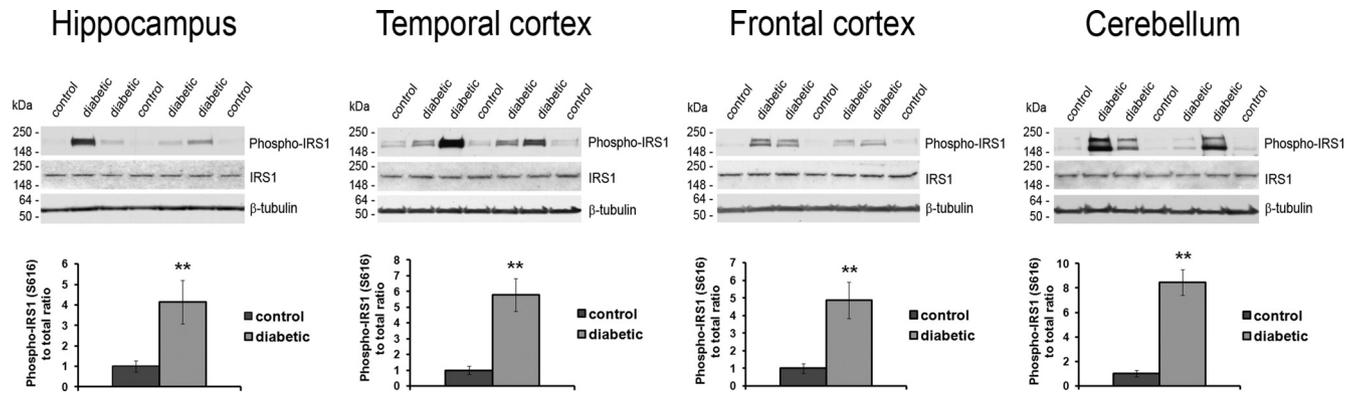
Figure 2. Altered IRS1 phosphorylation in the brain of the diabetic monkeys. Western blot analysis showing phospho-Ser616 and total protein levels for IRS1 in each of the four indicated brain regions. Quantitation of phospho-IRS1 normalized to the total protein level is given in the bottom four graphs for each region. β-Tubulin was used as a loading control. **$p < 0.01$.

treated monkeys did not receive their morning insulin therapy before blood sampling. Glucose levels obtained at this time point are also shown in Figure 1 [(2); insulin treatment withheld; 574 ± 59 mg glucose/dl in diabetic vs 65 ± 3 mg/dl in control monkeys, $p < 0.001$].

Diabetic and control monkeys were killed at intervals of 8, 16, and 20 weeks after treatment (see Materials and Methods; brain tissue was also collected from a single control animal killed at 4 weeks and a single diabetic animal killed at 12 weeks). The data presented in this study are pooled from animals killed at all time points after STZ or saline treatment. A *post hoc* statistical analysis of our findings argued that the *n* value at each time interval is too limited to draw additional interpretations across the time course (data not shown). Diabetic animals were treated with insulin the day they were killed, and glucose measurements of blood obtained during necropsy are shown in Figure 1 [(3); 330 ± 61 mg glucose/dl in diabetic vs 96 ± 7 mg/dl in control monkey, $p < 0.01$]. Throughout this study, we have examined regionally dissected hippocampus, frontal cortex, superior temporal cortex, and cerebellum obtained from frozen coronal-sectioned brain slabs.

Although the pathways by which DM may affect the brain are multifactorial, evidence exists in rodents that DM-driven insulin dysregulation and alterations in insulin signaling may directly affect tau phosphorylation (Sims-Robinson et al., 2010; El Khoury et al., 2014; Biessels and Reagan, 2015). Additionally, insulin-signaling pathway downregulation has been described in human AD brain, particularly within the hippocampus (Talbot et al., 2012). Given that endogenous insulin production was reduced greatly in this type 1 DM model (Kavanagh et al., 2011) and that twice-daily insulin treatment does not recapitulate the fine-tuned regulation of normal pancreatic insulin secretion (Chang and Schneider, 1971), we looked for evidence of insulin-signaling pathway alterations in the brains of the diabetic monkeys. From the regionally dissected frozen brain tissue, we examined the phosphorylation state of the IRS1 (Gual et al., 2005) to explore the role that insulin dysregulation may directly play in the DM-mediated effects. IRS1 acts as a molecular bottleneck for the insulin-signaling cascade and is initially activated via stimulation of insulin receptor by insulin (White, 2006). In each of the four brain regions examined, we found that the levels of the inhibitory phosphorylation of IRS1 at Ser616 were increased in the diabetic monkeys compared with control monkeys (Fig. 2; $p < 0.01$), whereas total IRS1 levels were unchanged (Fig. 2; $p > 0.05$). This finding is consistent with alterations in the insulin-signaling pathway suggestive of insulin resistance (Moloney et al.,

2010; Talbot et al., 2012) and argues that alterations in insulin signaling within the brain occurred in the type 1 DM monkeys.

We next assessed tau expression and tau protein phosphorylation status by Western blot analysis (Fig. 3). Total tau protein levels (detected with the DA9 antibody) and nonphosphorylated tau (detected with the tau1 antibody) were unchanged in the diabetic monkeys relative to controls (Fig. 3; $p > 0.05$). However, tau phosphorylation levels (detected with PHF-1 and CP13 antibodies) were increased in each region analyzed (Fig. 3; p values as indicated). A brain-wide increase in tau phosphorylation detected with tau phospho-epitope-specific antibodies is consistent with previous results in both type 1 DM (Planel et al., 2007; Ke et al., 2009; Jolivalt et al., 2010; Papon et al., 2013) and type 2 DM (Li et al., 2012; Jung et al., 2013) mouse models.

We next examined phosphatases and kinases that may contribute to a change in the phosphorylation pattern of tau in the diabetic monkey brain. An increase in tau phosphorylation in diabetic mouse brain has been attributed previously to a decrease in PP2A protein levels (Papon et al., 2013). Contrary to these findings in rodents, we did not detect a change in the levels of the catalytic domain of PP2A in any of the examined brain regions of the diabetic monkeys, nor were changes in the levels of PP2B seen (Fig. 3). Given that our findings suggest that a decrease in tau dephosphorylation may not contribute to an increase in phospho-tau in the diabetic monkey brain, we further examined potential tau kinases. We found an increase in an active form of ERK1/2 that can contribute to tau phosphorylation at both the PHF-1 and CP13 antibody epitope sites (Reynolds et al., 2000), in each examined brain region (Fig. 3; p values are indicated). Several reports have argued that ERK1/2 can phosphorylate tau (Drewes et al., 1992; Reynolds et al., 2000), although a direct role for ERK1/2 activity in phosphorylating tau is not universally supported (Noël et al., 2015). Total ERK1/2 protein levels did not change as a function of diabetic status (Fig. 3).

Similarly to what has been seen previously in a type 1 DM rodent model (Planel et al., 2007), we found an increase in an inhibitory phosphorylation at Ser9 in GSK3β without an increase in total GSK3β protein levels (Fig. 3; p values is indicated). This argues that GSK3β activity is downregulated in the diabetic monkeys and is therefore unlikely to contribute directly to increased tau phosphorylation. ERK1/2 activity can play a direct role in the downregulation of GSK3β (Wang et al., 2006), and upregulation of ERK1/2 combined with downregulation of GSK3β, as we detect in type 1 DM monkey brain, has been seen in human AD brain (Talbot et al., 2012). Protein levels of p35/p25 regulatory subunits of CDK5 and the catalytic domain of CDK5, an addi-

Hippocampus
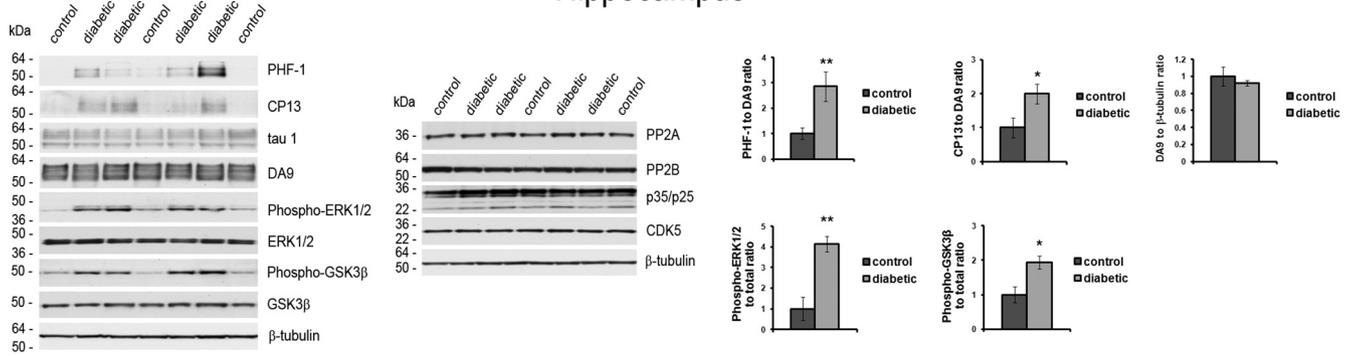
Temporal cortex
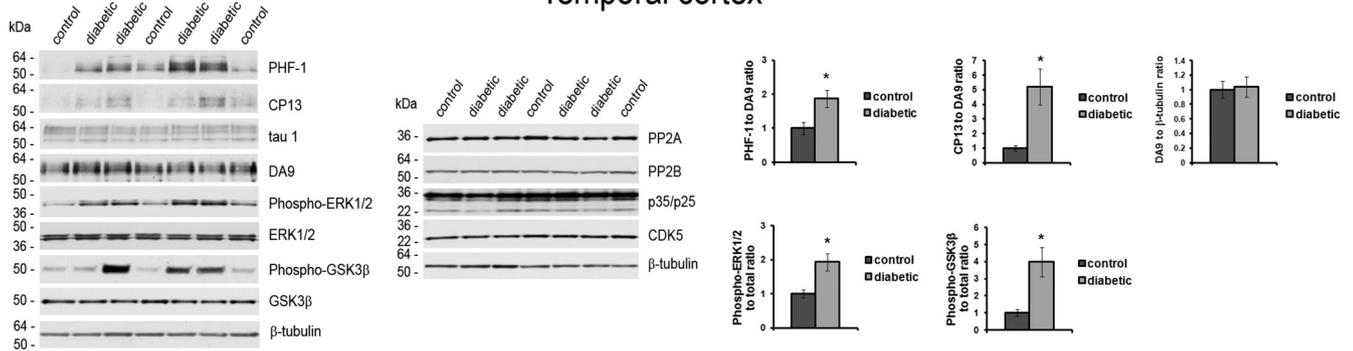
Frontal cortex
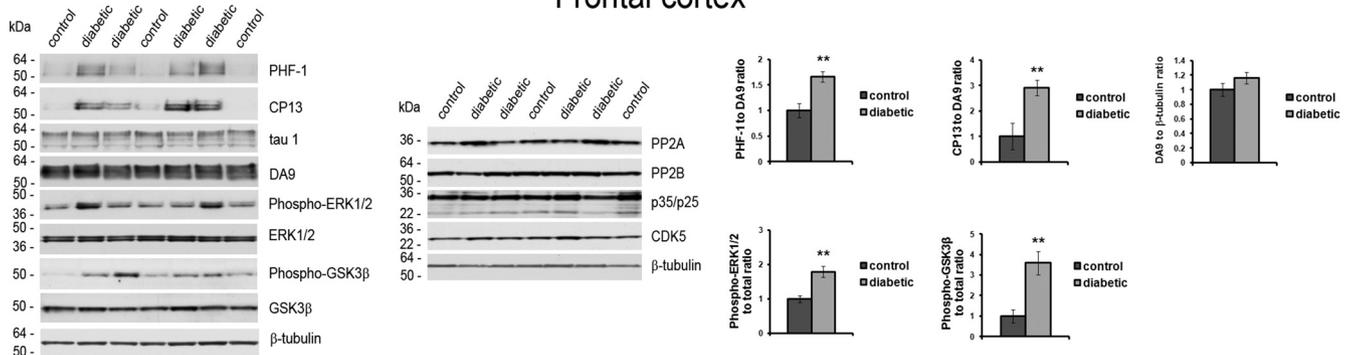
Cerebellum
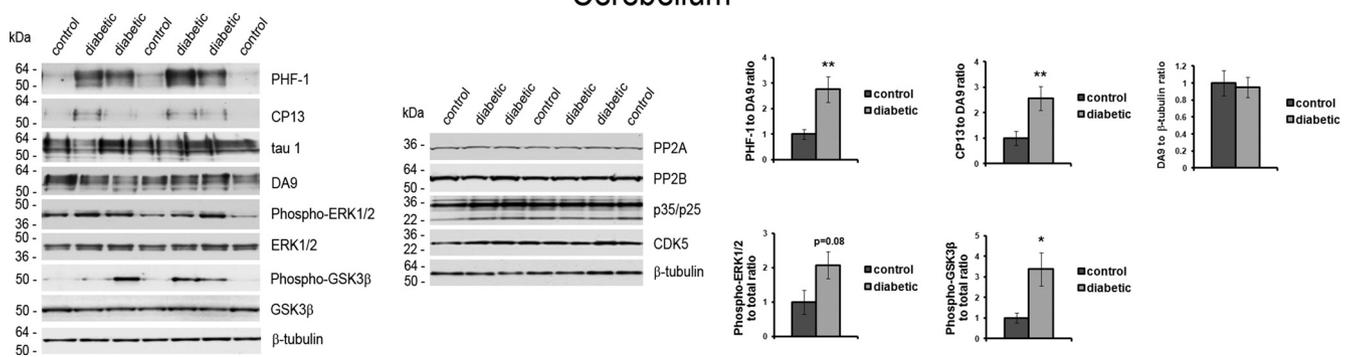
Figure 3. Increased tau phosphorylation throughout the brain in type 1 DM monkeys. Western blot analysis was performed on total protein homogenates prepared from tissue dissected from the indicated brain regions; representative panels are shown. On the left side, phospho-tau levels were determined using PHF-1 (phospho-Ser396/404) and CP13 (phospho-Ser202) antibodies (top panels). For comparison, total tau protein levels (detected with DA9 antibody) and non-phosphorylated tau (detected with tau1 antibody) are also shown. Western blots probed for phospho-ERK1/2 (phospho-Thr202/204), total ERK1/2, phospho-GSK3β (phospho-Ser9), total GSK3β, PP2A, PP2B, p35/p25 and the catalytic domain of CDK5 are shown. On the right side, quantitation of the PHF-1 and CP13 immunoreactivity normalized to total tau protein (DA9) and DA9 immunoreactivity normalized to β-tubulin is given in the top three graphs shown for each brain region. Quantitation of phospho-ERK1/2 and phospho-GSK3β levels normalized to the total protein level is given in the bottom two graphs for each region. β-tubulin was used as a loading control. *$p < 0.05$ and **$p < 0.01$.
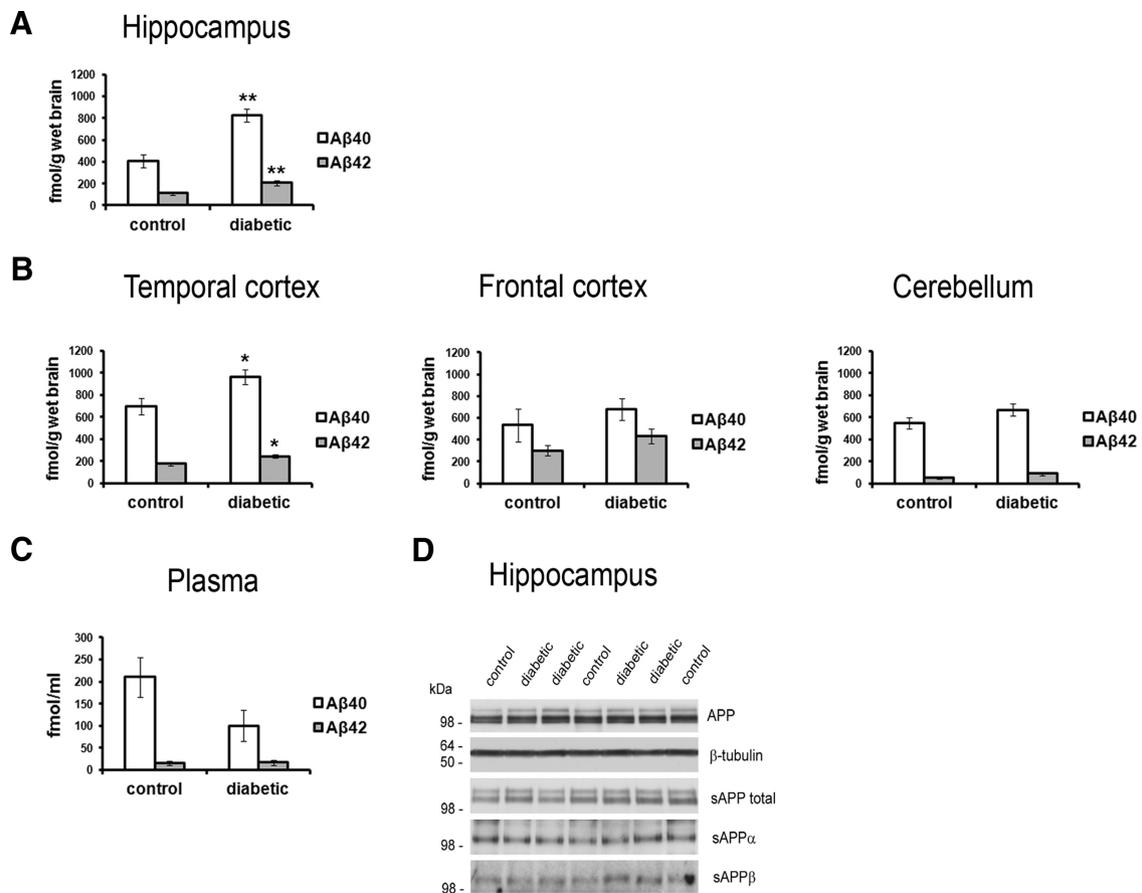
Figure 4. Increased Aβ levels in the hippocampus and temporal cortex in type 1 DM monkeys. $A\beta_{40}$ and $A\beta_{42}$ levels from each brain region were measured by sandwich ELISA (**A**, hippocampus; **B**, temporal cortex, frontal cortex, and cerebellum). **C**, $A\beta_{40}$ and $A\beta_{42}$ levels determined by sandwich ELISA in blood plasma collected at the time of death. Additional APP metabolites as indicated were detected in brain by Western blot analysis (**D**, hippocampus; data not shown for additional brain regions); β-tubulin was used as a loading control. $*p < 0.05$; $**p < 0.01$.

tional potential tau kinase, were not altered in the diabetic monkeys (Fig. 3). Therefore, our findings suggest a role for ERK1/2 activity increasing tau phosphorylation throughout the diabetic brain.

However, a brain-wide increase in phosphorylated tau is not consistent with the regional pattern of tau pathology that develops during AD, in which temporal lobe structures, including the hippocampus, are affected earlier and more severely (Braak and Braak, 1995; Buee et al., 2000). Additionally, although increased tau phosphorylation has been suggested as a molecular link between DM and AD risk (Planel et al., 2007; Ke et al., 2009; Jolivalt et al., 2010; Li et al., 2012; Jung et al., 2013; Papon et al., 2013), tau pathology in AD is likely to be promoted at least in part by changes in Aβ levels (Götz et al., 2001; Lewis et al., 2001). Therefore, we examined endogenous Aβ levels by sandwich ELISA within these brain regions. In the diabetic monkeys compared with control monkeys, soluble Aβ levels approximately doubled in the hippocampus ($A\beta_{40}$, 2.03 ± 0.14 and $A\beta_{42}$, 1.86 ± 0.20 times control levels; $p < 0.01$; Fig. 4A) and increased by ~40% in the temporal cortex ($A\beta_{40}$, 1.38 ± 0.09 and $A\beta_{42}$, 1.39 ± 0.08 times control levels; $p < 0.05$; Fig. 4B). In contrast to these temporal lobe structures, the frontal cortex and cerebellum did not show significant changes in Aβ levels (Fig. 4B; $p > 0.05$). As a comparison with brain, blood plasma Aβ levels were unchanged in the diabetic monkeys (Fig. 4C; $p > 0.05$).

Cerebral Aβ levels are dependent on the rate of cellular Aβ production from APP, as well as the efficacy of Aβ clearance by proteolysis and Aβ transport to and from the periphery (Deane et

al., 2009). Levels of APP and the highly stable sAPP fragments (Morales-Corraliza et al., 2009) were not changed significantly in any of the brain regions, including the levels of the β-secretase cleaved sAPPβ fragment (Fig. 4D, hippocampus; $p > 0.05$; data not shown for additional brain regions), arguing that upregulated β-secretase cleavage leading to increased Aβ production from the APP protein does not occur in the brain of diabetic monkeys. Alternatively, elevated cerebral Aβ levels may be attributable to a change in the transport of Aβ across the blood–brain barrier (BBB). Aβ transport into the brain is mediated primarily by RAGE (Deane et al., 2003), whereas LRP1 mediates transport from the brain to the periphery (Sagare et al., 2007). The formation and accumulation of advanced glycation end products (AGEs), which comprise a heterogeneous group of sugars conjugated to proteins, lipids, and nucleic acids that are the ligands for RAGE, occur during normal aging, with DM greatly exacerbating AGE modifications with subsequent changes in RAGE expression (Brownlee, 1995). However, we found that RAGE expression levels were not significantly different between the diabetic and control monkeys (Fig. 5A; $p > 0.05$), nor were changes in RAGE expression seen in the liver (Fig. 5C; $p > 0.05$) or of a secretory form of RAGE in the blood plasma (Fig. 5D; $p > 0.05$). Similarly, LRP1 expression did not change in the brain (Fig. 5A; $p > 0.05$), in the liver (Fig. 5C; $p > 0.05$), or, in its soluble form, in blood plasma (Fig. 5D; $p > 0.05$). Together, these findings, and the lack of a change in blood plasma Aβ levels (Fig. 4C), suggest that increased Aβ production or altered Aβ transport across the BBB are unlikely to be the primary mechanism underlying the in-

A

B

C

D
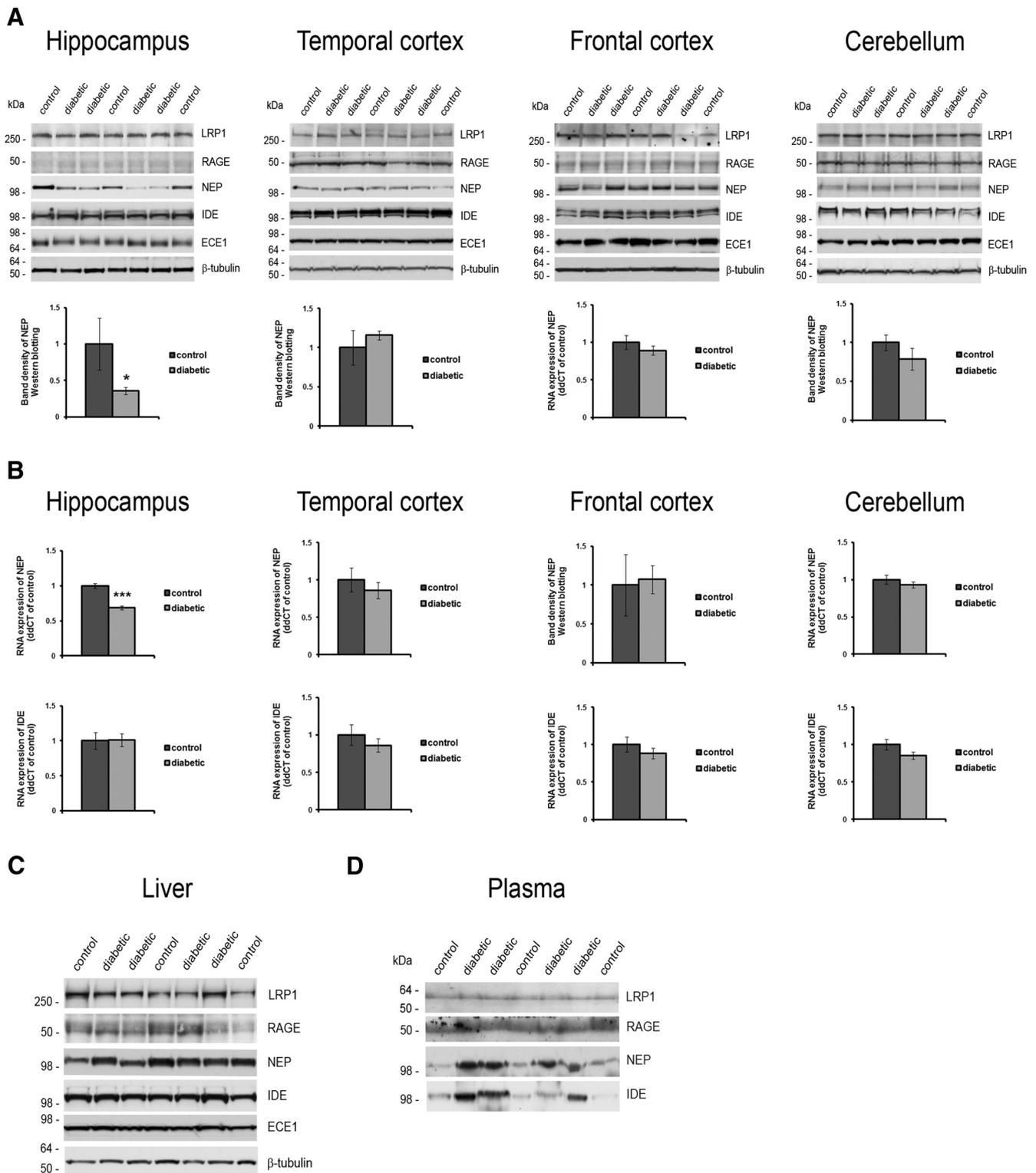
Figure 5. Reduced hippocampal NEP expression in the diabetic monkeys. ***A***, Western blot analysis showing LRP1, RAGE, NEP, IDE, and ECE1 protein expression and graphs showing the quantitation of NEP protein levels in each of the four indicated brain regions. ***B***, mRNA levels for NEP (top row) and IDE (bottom row) as determined by qPCR analysis. In ***C***, LRP1, RAGE, NEP, IDE, and ECE1 protein expression in the liver is shown. β-Tubulin was used as a loading control. ***D***, Blood plasma collected at the time of death probed for secreted LRP1, RAGE, NEP and IDE. Equal blood plasma volumes were loaded. $*p < 0.05$; $***p < 0.001$.

creases in Aβ levels seen in the hippocampus and temporal cortex of diabetic monkeys.

NEP, IDE, and ECE1 are important brain Aβ-degrading proteases (Qiu et al., 1998; Iwata et al., 2000; Eckman et al., 2001) that also contribute to the regulation of peripheral insulin (Johnson et

al., 1999; Farris et al., 2003). Plasma NEP levels have been shown to increase in mice after diet-induced insulin resistance, and a similar plasma NEP increase was seen with insulin resistance and other markers of metabolic syndrome in humans (Standeven et al., 2011). In the monkeys, DM induced a robust increase in both

plasma NEP (2.66 ± 0.41 times control levels; $p < 0.01$) and plasma IDE (3.51 ± 0.68 times control levels; $p < 0.05$; Fig. 5D), although the levels of NEP, IDE, and ECE1 were unchanged in liver homogenates of the diabetic monkeys (Fig. 5C; $p > 0.05$). However, an increase in peripheral NEP expression is unlikely to affect brain Aβ levels (Walker et al., 2013), and the effect of DM on brain NEP, IDE, or ECE1 is not well understood and may differ from the response in the periphery.

Indeed, in contrast to the blood plasma increase in protein levels, NEP levels in the hippocampus were significantly decreased in the diabetic monkeys (to 0.36 ± 0.05 of control; $p < 0.05$; Fig. 5A; NEP panel and graph, hippocampus). In the brain, this decrease in NEP was confined to the hippocampus, with frontal cortex, temporal cortex, and cerebellum not showing a significant change in NEP protein levels (Fig. 5A; NEP panels and graphs, temporal cortex, frontal cortex, and cerebellum; $p > 0.05$). Hippocampal NEP mRNA levels were also reduced in the diabetic monkeys to 0.69 ± 0.06 of control levels ($p < 0.001$), whereas no differences were observed in the other brain regions (top graphs in Fig. 5B; $p > 0.05$), arguing that a reduction in NEP gene expression underlies a DM-induced reduction in hippocampal NEP protein levels. IDE and ECE1 protein levels were unchanged in all four brain regions examined (Fig. 5A; $p > 0.05$). Consistent with a lack of IDE protein level changes, IDE mRNA levels were found to be unchanged in the diabetic brain (Fig. 5B, bottom graphs; $p > 0.05$). In summary, our examination of APP/APP metabolite expression and Aβ catabolic proteins argues that a localized reduction in NEP expression in the diabetic primate brain underlies an increase in Aβ in the hippocampus and adjacent temporal lobe structures.

Discussion

Given the rapidly increasing prevalence of DM (www.cdc.gov/diabetes/pubs/pdf/DiabetesReportCard.pdf) and its potential relationship to cognitive decline and dementia (Akomolafe et al., 2006; Biessels et al., 2006; Sims-Robinson et al., 2010; McCrimmon et al., 2012), understanding how DM contributes to AD is of critical public health importance and is necessary to determine the appropriate clinical interventions that will mitigate AD risk in this population. In this study, we have identified biochemical changes occurring in the brains of a nonhuman primate model of type 1 DM that are consistent with changes in insulin signaling, as well as changes in both tau and Aβ metabolism that are likely to contribute to the risk of developing AD pathology and clinical manifestation of the disease over time.

We found that the levels of an inhibitory phosphorylation of IRS1 were increased in the brains of the insulin-treated diabetic monkeys, suggesting that the insulin-signaling pathway was altered as has been reported in AD and MCI brain (Talbot et al., 2012). Although type 1 and type 2 DM have distinct initial etiologies, dysregulation of insulin occurs in both diseases. For type 1 diabetics, severe hypoinsulinemia attributable to pancreatic β-cell loss necessitates life-long exogenous insulin therapy (McCrimmon and Sherwin, 2010). Type 2 DM is driven by peripheral insulin resistance, which initially leads to compensatory hyperinsulinemia in an attempt to maintain glucose homeostasis (Festa et al., 2006). However, type 2 DM frequently progresses to the point at which the pancreas fails to produce sufficient insulin ("pancreatic burnout"), resulting in both insulin resistance and hypoinsulinemia and necessitating insulin therapy (DeFronzo, 2004). Like type 2 DM, type 1 DM patients may also show signs of the insulin resistance over time (Greenbaum, 2002). Thus, although human epidemiology most clearly links type 2 DM with

increased risk of AD (Akomolafe et al., 2006; Biessels et al., 2006; Sims-Robinson et al., 2010; McCrimmon et al., 2012), dysregulation of insulin and therefore insulin signaling in the brain is a commonality for both type 1 and type 2 DM, and this is likely to affect the brain (Talbot et al., 2012; Biessels and Reagan, 2015). Our findings are consistent with the hypothesis that dysregulation of IRS1 is likely attributable to changes in the insulin signaling pathway that may result in downstream effects on NEP and Aβ, and ERK1/2 and tau. The insulin-signaling cascade expands through a number of kinases, including ERK1/2, and it is likely that direct effects of insulin in the brain are responsible for the tau phosphorylation changes we see, as have been proposed by others based on rodent findings. Although the changes in phospho-epitope levels in the diabetic monkeys does not include AD-like tau pathology, such as neurofibrillary tangle formation, a modest change in tau phosphorylation has the potential to contribute to pathological tau changes when extended over many years and in context of additional AD drivers, such as increased brain Aβ. Moreover, increased tau phosphorylation at Ser202 (detected by the CP13 antibody) and Ser396/Ser404 (detected by the PHF-1 antibody), as we see the diabetic monkeys, has been reported in the brains of type 2 DM patients (Liu et al., 2009) and is seen robustly in paired-helical filaments and neurofibrillary tangles in AD (Kimura et al., 1996). This is consistent with DM leading to increased tau phosphorylation at AD pathology-relevant sites.

Relatively small changes in brain Aβ levels early in life appear to be sufficient to lead to early AD pathology in humans, suggesting that an increase in brain Aβ levels in DM may be disease relevant if extended for many years. An extra copy of the *App* gene in early onset AD kindreds and in individuals with Down syndrome inevitably leads to disease, including both Aβ and tau pathology (Rovelet-Lecrux et al., 2006; Sleegers et al., 2006). In these individuals, the additional *App* gene is likely to only increase brain Aβ production levels by one-half, less than the doubling of Aβ seen in the hippocampus in the diabetic monkeys and similar to that seen in the temporal cortex.

Unlike in the periphery, in which Aβ is cleared rapidly by the liver and also excreted into the urine (Ghiso et al., 2004), cerebral Aβ clearance is dependent on local degradation and transport across the BBB. Our findings suggest that, of the proteins known to play a prominent role in modulating brain Aβ levels, NEP is uniquely downregulated in the hippocampus of a nonhuman primate model of type 1 DM. In addition, treatment with NEP inhibitors leads to an increase in Aβ levels in the brain (Iwata et al., 2000), and NEP-deficient mice have elevated brain Aβ levels (Iwata et al., 2001), which promotes Aβ pathology in APP transgenic mice (Farris et al., 2007). A DM-induced reduction in NEP expression is likely to lead to the increase in Aβ seen within the hippocampus, with the smaller increase in Aβ seen in overlying temporal cortex consistent with the synaptic interconnectivity of the temporal lobe and exchange of APP metabolites, including Aβ, between these two regions (Harris et al., 2010). Our observations are also consistent with the previous finding that genetic deletion of NEP results in the greatest increase in Aβ levels within the hippocampus, with cortical regions showing a more modest increase, and the cerebellum even less of a change (Iwata et al., 2001). Multiple lines of evidence suggest that NEP expression in the brain correlates with AD risk and pathology: postmortem studies suggest that NEP levels are reduced in the brain with aging (Caccamo et al., 2005; Hellström-Lindahl et al., 2008) and also reduced in tissue with AD pathology (Yasojima et al., 2001), whereas IDE and ECE1 expression are unchanged (Wang et al.,

2010). Our findings implicate DM as a driver of brain NEP down-regulation, which could promote subsequent Aβ pathology.

In conclusion, our regional analysis of type 1 DM monkey brain suggests multiple biochemical connections that link DM to AD. A localized decrease in NEP expression and an increase in Aβ occurs in the temporal lobe brain structures that are at the earliest risk in AD (Braak and Braak, 1995). DM in this model also led to alterations in the insulin-signaling pathway that are likely to be responsible for an increase in ERK1/2 activity and that likely contributed to an increase in tau phosphorylation. Better understanding the interplay between DM and NEP expression may suggest DM management strategies that limit the effect of the disease on brain expression of NEP, reducing the subsequent risk for AD-related neuropathology.

References

Agresti A (2007) An introduction to categorical data analysis, Ed 2. New York: Wiley.

Akomolafe A, Beiser A, Meigs JB, Au R, Green RC, Farrer LA, Wolf PA, Seshadri S (2006) Diabetes mellitus and risk of developing Alzheimer disease: results from the Framingham Study. Arch Neurol 63:1551–1555. CrossRef Medline

Alldred MJ, Che S, Ginsberg SD (2009) Terminal continuation (TC) RNA amplification without second strand synthesis. J Neurosci Methods 177: 381–385. CrossRef Medline

Alldred MJ, Duff KE, Ginsberg SD (2012) Microarray analysis of CA1 pyramidal neurons in a mouse model of tauopathy reveals progressive synaptic dysfunction. Neurobiol Dis 45:751–762. CrossRef Medline

Biessels GJ, Reagan LP (2015) Hippocampal insulin resistance and cognitive dysfunction. Nat Rev Neurosci 16:660–671. CrossRef Medline

Biessels GJ, Staekenborg S, Brunner E, Brayne C, Scheltens P (2006) Risk of dementia in diabetes mellitus: a systematic review. Lancet Neurol 5: 64–74. CrossRef Medline

Braak H, Braak E (1995) Staging of Alzheimer's disease-related neurofibrillary changes. Neurobiol Aging 16:271–278; discussion 278–284. Medline

Brownlee M (1995) Advanced protein glycosylation in diabetes and aging. Annu Rev Med 46:223–234. CrossRef Medline

Buée L, Bussière T, Buée-Scherrer V, Delacourte A, Hof PR (2000) Tau protein isoforms, phosphorylation and role in neurodegenerative disorders. Brain Res Brain Res Rev 33:95–130. CrossRef Medline

Caccamo A, Oddo S, Sugarman MC, Akbari Y, LaFerla FM (2005) Age- and region-dependent alterations in Aβ-degrading enzymes: implications for Aβ-induced disorders. Neurobiol Aging 26:645–654. CrossRef Medline

Chang AY, Schneider DI (1971) Hepatic enzyme activities in streptozotocin-diabetic rats before and after insulin treatment. Diabetes 20: 71–77. CrossRef Medline

Chen Y, Zhao Y, Dai CL, Liang Z, Run X, Iqbal K, Liu F, Gong CX (2014a) Intranasal insulin restores insulin signaling, increases synaptic proteins, and reduces Aβ level and microglia activation in the brains of 3xTg-AD mice. Exp Neurol 261:610–619. CrossRef Medline

Chen Y, Run X, Liang Z, Zhao Y, Dai CL, Iqbal K, Liu F, Gong CX (2014b) Intranasal insulin prevents anesthesia-induced hyperphosphorylation of tau in 3xTg-AD mice. Front Aging Neurosci 6:100. CrossRef Medline

Claxton A, Baker LD, Hanson A, Trittschuh EH, Cholerton B, Morgan A, Callaghan M, Arbuckle M, Behl C, Craft S (2015) Long-acting intranasal insulin detemir improves cognition for adults with mild cognitive impairment or early-stage Alzheimer's disease dementia. J Alzheimers Dis [Erratum (2015) 45:1269–1270] 44:897–906. CrossRef Medline

Craft S, Baker LD, Montine TJ, Minoshima S, Watson GS, Claxton A, Arbuckle M, Callaghan M, Tsai E, Plymate SR, Green PS, Leverenz J, Cross D, Gerton B (2012) Intranasal insulin therapy for Alzheimer disease and amnestic mild cognitive impairment: a pilot clinical trial. Arch Neurol 69:29–38. CrossRef Medline

de la Monte SM, Tong M (2014) Brain metabolic dysfunction at the core of Alzheimer's disease. Biochem Pharmacol 88:548–559. CrossRef Medline

Deane R, Du Yan S, Submamaryan RK, LaRue B, Jovanovic S, Hogg E, Welch D, Manness L, Lin C, Yu J, Zhu H, Ghiso J, Frangione B, Stern A, Schmidt AM, Armstrong DL, Arnold B, Liliensiek B, Nawroth P, Hofman F, Kindy M, Stern D, Zlokovic B (2003) RAGE mediates β-amyloid peptide

transport across the blood-brain barrier and accumulation in brain. Nat Med 9:907–913. CrossRef Medline

Deane R, Bell RD, Sagare A, Zlokovic BV (2009) Clearance of β-amyloid peptide across the blood-brain barrier: implication for therapies in Alzheimer's disease. CNS Neurol Disord Drug Targets 8:16–30. CrossRef Medline

De Felice FG, Lourenco MV (2015) Brain metabolic stress and neuroinflammation at the basis of cognitive impairment in Alzheimer's disease. Front Aging Neurosci 7:94. CrossRef Medline

DeFronzo RA (2004) Pathogenesis of type 2 diabetes mellitus. Med Clin North Am 88:787–835, ix. Medline

Devi L, Alldred MJ, Ginsberg SD, Ohno M (2012) Mechanisms underlying insulin deficiency-induced acceleration of β-amyloidosis in a mouse model of Alzheimer's disease. PLoS One 7:e32792. CrossRef Medline

Drewes G, Lichtenberg-Kraag B, Döring F, Mandelkow EM, Biernat J, Goris J, Dorée M, Mandelkow E (1992) Mitogen activated protein (MAP) kinase transforms tau protein into an Alzheimer-like state. EMBO J 11: 2131–2138. Medline

Eckman EA, Reed DK, Eckman CB (2001) Degradation of the Alzheimer's β-amyloid peptide by endothelin- converting enzyme. J Biol Chem 276: 24540–24548. CrossRef Medline

El Khoury NB, Gratuze M, Papon MA, Bretteville A, Planel E (2014) Insulin dysfunction and Tau pathology. Front Cell Neurosci 8:22. CrossRef Medline

Farris W, Mansourian S, Chang Y, Lindsley L, Eckman EA, Frosch MP, Eckman CB, Tanzi RE, Selkoe DJ, Guenette S (2003) Insulin-degrading enzyme regulates the levels of insulin, β-amyloid protein, and the β-amyloid precursor protein intracellular domain in vivo. Proc Natl Acad Sci U S A 100:4162–4167. CrossRef Medline

Farris W, Schütz SG, Cirrito JR, Shankar GM, Sun X, George A, Leissring MA, Walsh DM, Qiu WQ, Holtzman DM, Selkoe DJ (2007) Loss of neprilysin function promotes amyloid plaque formation and causes cerebral amyloid angiopathy. Am J Pathol 171:241–251. CrossRef Medline

Festa A, Williams K, Tracy RP, Wagenknecht LE, Haffner SM (2006) Progression of plasminogen activator inhibitor-1 and fibrinogen levels in relation to incident type 2 diabetes. Circulation 113:1753–1759. CrossRef Medline

Garcíia-Casares N, Jorge RE, García-Arnés JA, Acion L, Berthier ML, Gonzalez-Alegre P, Nabrozidis A, Gutiérrez A, Ariza MJ, Rioja J, González-Santos P (2014) Cognitive dysfunctions in middle-aged type 2 diabetic patients and neuroimaging correlations: a cross-sectional study. J Alzheimers Dis 42:1337–1346. CrossRef Medline

Ghiso J, Shayo M, Calero M, Ng D, Tomidokoro Y, Gandy S, Rostagno A, Frangione B (2004) Systemic catabolism of Alzheimer's Aβ40 and Aβ42. J Biol Chem 279:45897–45908. CrossRef Medline

Ginsberg SD, Alldred MJ, Counts SE, Cataldo AM, Neve RL, Jiang Y, Wuu J, Chao MV, Mufson EJ, Nixon RA, Che S (2010) Microarray analysis of hippocampal CA1 neurons implicates early endosomal dysfunction during Alzheimer's disease progression. Biol Psychiatry 68:885–893. CrossRef Medline

Götz J, Chen F, van Dorpe J, Nitsch RM (2001) Formation of neurofibrillary tangles in P301l tau transgenic mice induced by Aβ42 fibrils. Science 293:1491–1495. CrossRef Medline

Greenbaum CJ (2002) Insulin resistance in type 1 diabetes. Diabetes Metab Res Rev 18:192–200. CrossRef Medline

Gual P, Le Marchand-Brustel Y, Tanti JF (2005) Positive and negative regulation of insulin signaling through IRS-1 phosphorylation. Biochimie 87:99–109. CrossRef Medline

Harris JA, Devidze N, Verret L, Ho K, Halabisky B, Thwin MT, Kim D, Hamto P, Lo I, Yu GQ, Palop JJ, Masliah E, Mucke L (2010) Transsynaptic progression of β-amyloid-induced neuronal dysfunction within the entorhinal-hippocampal network. Neuron 68:428–441. CrossRef Medline

Hellström-Lindahl E, Ravid R, Nordberg A (2008) Age-dependent decline of neprilysin in Alzheimer's disease and normal brain: inverse correlation with Aβ levels. Neurobiol Aging 29:210–221. CrossRef Medline

Hölscher C (2014) First clinical data of the neuroprotective effects of nasal insulin application in patients with Alzheimer's disease. Alzheimers Dement 10:S33–S37. CrossRef Medline

Iwata N, Tsubuki S, Takaki Y, Watanabe K, Sekiguchi M, Hosoki E, Kawashima-Morishima M, Lee HJ, Hama E, Sekine-Aizawa Y, Saido TC (2000) Identification of the major Aβ1-42-degrading catabolic pathway

in brain parenchyma: suppression leads to biochemical and pathological deposition. Nat Med 6:143–150. CrossRef Medline

Iwata N, Tsubuki S, Takaki Y, Shirotani K, Lu B, Gerard NP, Gerard C, Hama E, Lee HJ, Saido TC (2001) Metabolic regulation of brain Aβ by neprilysin. Science 292:1550–1552. CrossRef Medline

Johnson GD, Stevenson T, Ahn K (1999) Hydrolysis of peptide hormones by endothelin-converting enzyme-1. A comparison with neprilysin. J Biol Chem 274:4053–4058. CrossRef Medline

Jolivalt CG, Hurford R, Lee CA, Dumaop W, Rockenstein E, Masliah E (2010) Type 1 diabetes exaggerates features of Alzheimer's disease in APP transgenic mice. Exp Neurol 223:422–431. CrossRef Medline

Jung HJ, Kim YJ, Eggert S, Chung KC, Choi KS, Park SA (2013) Age-dependent increases in tau phosphorylation in the brains of type 2 diabetic rats correlate with a reduced expression of p62. Exp Neurol 248:441–450. CrossRef Medline

Kavanagh K, Flynn DM, Nelson C, Zhang L, Wagner JD (2011) Characterization and validation of a streptozotocin-induced diabetes model in the vervet monkey. J Pharmacol Toxicol Methods 63:296–303. CrossRef Medline

Ke YD, Delerue F, Gladbach A, Götz J, Ittner LM (2009) Experimental diabetes mellitus exacerbates tau pathology in a transgenic mouse model of Alzheimer's disease. PLoS One 4:e7917. CrossRef Medline

Kimura T, Ono T, Takamatsu J, Yamamoto H, Ikegami K, Kondo A, Hasegawa M, Ihara Y, Miyamoto E, Miyakawa T (1996) Sequential changes of tau-site-specific phosphorylation during development of paired helical filaments. Dementia 7:177–181. Medline

Lewis J, Dickson DW, Lin WL, Chisholm L, Corral A, Jones G, Yen SH, Sahara N, Skipper L, Yager D, Eckman C, Hardy J, Hutton M, McGowan E (2001) Enhanced neurofibrillary degeneration in transgenic mice expressing mutant tau and APP. Science 293:1487–1491. CrossRef Medline

Li J, Deng J, Sheng W, Zuo Z (2012) Metformin attenuates Alzheimer's disease-like neuropathology in obese, leptin-resistant mice. Pharmacol Biochem Behav 101:564–574. CrossRef Medline

Liu Y, Liu F, Grundke-Iqbal I, Iqbal K, Gong CX (2009) Brain glucose transporters, O-GlcNAcylation and phosphorylation of tau in diabetes and Alzheimer's disease. J Neurochem 111:242–249. CrossRef Medline

Mathews PM, Jiang Y, Schmidt SD, Grbovic OM, Mercken M, Nixon RA (2002) Calpain activity regulates the cell surface distribution of amyloid precursor protein. Inhibition of calpains enhances endosomal generation of β-cleaved C-terminal APP fragments. J Biol Chem 277:36415–36424. CrossRef Medline

McCrimmon RJ, Sherwin RS (2010) Hypoglycemia in type 1 diabetes. Diabetes 59:2333–2339. CrossRef Medline

McCrimmon RJ, Ryan CM, Frier BM (2012) Diabetes and cognitive dysfunction. Lancet 379:2291–2299. CrossRef Medline

Moloney AM, Griffin RJ, Timmons S, O'Connor R, Ravid R, O'Neill C (2010) Defects in IGF-1 receptor, insulin receptor and IRS-1/2 in Alzheimer's disease indicate possible resistance to IGF-1 and insulin signalling. Neurobiol Aging 31:224–243. CrossRef Medline

Morales-Corraliza J, Mazzella MJ, Berger JD, Diaz NS, Choi JH, Levy E, Matsuoka Y, Planel E, Mathews PM (2009) In vivo turnover of tau and APP metabolites in the brains of wild-type and Tg2576 mice: greater stability of sAPP in the β-amyloid depositing mice. PLoS One 4:e7134. CrossRef Medline

Morales-Corraliza J, Schmidt SD, Mazzella MJ, Berger JD, Wilson DA, Wesson DW, Jucker M, Levy E, Nixon RA, Mathews PM (2013) Immunization targeting a minor plaque constituent clears β-amyloid and rescues behavioral deficits in an Alzheimer's disease mouse model. Neurobiol Aging 34:137–145. CrossRef Medline

Needham BE, Wlodek ME, Ciccotosto GD, Fam BC, Masters CL, Proietto J, Andrikopoulos S, Cappai R (2008) Identification of the Alzheimer's disease amyloid precursor protein (APP) and its homologue APLP2 as essential modulators of glucose and insulin homeostasis and growth. J Pathol 215:155–163. CrossRef Medline

Nishitomi K, Sakaguchi G, Horikoshi Y, Gray AJ, Maeda M, Hirata-Fukae C, Becker AG, Hosono M, Sakaguchi I, Minami SS, Nakajima Y, Li HF, Takeyama C, Kihara T, Ota A, Wong PC, Aisen PS, Kato A, Kinoshita N, Matsuoka Y (2006) BACE1 inhibition reduces endogenous Aβ and alters APP processing in wild-type mice. J Neurochem 99:1555–1563. CrossRef Medline

Noël A, Poitras I, Julien J, Petry FR, Morin F, Charron J, Planel E (2015)

ERK (MAPK) does not phosphorylate tau under physiological conditions in vivo or in vitro. Neurobiol Aging 36:901–902. CrossRef Medline

Papon MA, El Khoury NB, Marcouiller F, Julien C, Morin F, Bretteville A, Petry FR, Gaudreau S, Amrani A, Mathews PM, Hébert SS, Planel E (2013) Deregulation of protein phosphatase 2A and hyperphosphorylation of tau protein following onset of diabetes in NOD mice. Diabetes 62:609–617. CrossRef Medline

Planel E, Tatebayashi Y, Miyasaka T, Liu L, Wang L, Herman M, Yu WH, Luchsinger JA, Wadzinski B, Duff KE, Takashima A (2007) Insulin dysfunction induces in vivo tau hyperphosphorylation through distinct mechanisms. J Neurosci 27:13635–13648. CrossRef Medline

Qiu WQ, Walsh DM, Ye Z, Vekrellis K, Zhang J, Podlisny MB, Rosner MR, Safavi A, Hersh LB, Selkoe DJ (1998) Insulin-degrading enzyme regulates extracellular levels of β-amyloid protein by degradation. J Biol Chem 273:32730–32738. CrossRef Medline

Rdzak GM, Abdelghany O (2014) Does insulin therapy for type 1 diabetes mellitus protect against Alzheimer's disease? Pharmacotherapy 34:1317–1323. CrossRef Medline

Reynolds CH, Betts JC, Blackstock WP, Nebreda AR, Anderton BH (2000) Phosphorylation sites on tau identified by nanoelectrospray mass spectrometry: differences in vitro between the mitogen-activated protein kinases ERK2, c-Jun N-terminal kinase and P38, and glycogen synthase kinase-3β. J Neurochem 74:1587–1595. Medline

Rovelet-Lecrux A, Hannequin D, Raux G, Le Meur N, Laquerrière A, Vital A, Dumanchin C, Feuillette S, Brice A, Vercelletto M, Dubas F, Frebourg T, Campion D (2006) APP locus duplication causes autosomal dominant early-onset Alzheimer disease with cerebral amyloid angiopathy. Nat Genet 38:24–26. CrossRef Medline

Sagare A, Deane R, Bell RD, Johnson B, Hamm K, Pendu R, Marky A, Lenting PJ, Wu Z, Zarcone T, Goate A, Mayo K, Perlmutter D, Coma M, Zhong Z, Zlokovic BV (2007) Clearance of β-amyloid by circulating lipoprotein receptors. Nat Med 13:1029–1031. CrossRef Medline

Saisho Y, Manesso E, Butler AE, Galasso R, Kavanagh K, Flynn M, Zhang L, Clark P, Gurlo T, Toffolo GM, Cobelli C, Wagner JD, Butler PC (2011) Ongoing β-cell turnover in adult nonhuman primates is not adaptively increased in streptozotocin-induced diabetes. Diabetes 60:848–856. CrossRef Medline

Schmidt SD, Nixon RA, Mathews PM (2012a) Tissue processing prior to analysis of Alzheimer's disease associated proteins and metabolites, including Aβ. Methods Mol Biol 849:493–506. CrossRef Medline

Schmidt SD, Mazzella MJ, Nixon RA, Mathews PM (2012b) Aβ measurement by enzyme-linked immunosorbent assay. Methods Mol Biol 849:507–527. CrossRef Medline

Sims-Robinson C, Kim B, Rosko A, Feldman EL (2010) How does diabetes accelerate Alzheimer disease pathology? Nat Rev Neurol 6:551–559. CrossRef Medline

Sleegers K, Brouwers N, Gijselinck I, Theuns J, Goossens D, Wauters J, Del-Favero J, Cruts M, van Duijn CM, Van Broeckhoven C (2006) APP duplication is sufficient to cause early onset Alzheimer's dementia with cerebral amyloid angiopathy. Brain 129:2977–2983. CrossRef Medline

Soleilhac JM, Lafuma C, Porcher JM, Auburtin G, Roques BP (1996) Characterization of a soluble form of neutral endopeptidase-24.11 (EC 3.4.24.11) in human serum: enhancement of its activity in serum of underground miners exposed to coal dust particles. Eur J Clin Invest 26:1011–1017. CrossRef Medline

Standeven KF, Hess K, Carter AM, Rice GI, Cordell PA, Balmforth AJ, Lu B, Scott DJ, Turner AJ, Hooper NM, Grant PJ (2011) Neprilysin, obesity and the metabolic syndrome. Int J Obes (Lond) 35:1031–1040. CrossRef Medline

Szendrei GI, Lee VM, Otvos L Jr (1993) Recognition of the minimal epitope of monoclonal antibody Tau-1 depends upon the presence of a phosphate group but not its location. J Neurosci Res 34:243–249. CrossRef Medline

Takeda S, Sato N, Uchio-Yamada K, Sawada K, Kunieda T, Takeuchi D, Kurinami H, Shinohara M, Rakugi H, Morishita R (2010) Diabetes-accelerated memory dysfunction via cerebrovascular inflammation and Aβ deposition in an Alzheimer mouse model with diabetes. Proc Natl Acad Sci U S A 107:7036–7041. CrossRef Medline

Talbot K, Wang HY, Kazi H, Han LY, Bakshi KP, Stucky A, Fuino RL, Kawaguchi KR, Samoyedny AJ, Wilson RS, Arvanitakis Z, Schneider JA, Wolf BA, Bennett DA, Trojanowski JQ, Arnold SE (2012) Demonstrated brain insulin resistance in Alzheimer's disease patients is associated with

IGF-1 resistance, IRS-1 dysregulation, and cognitive decline. J Clin Invest 122:1316–1338. CrossRef Medline

Walker JR, Pacoma R, Watson J, Ou W, Alves J, Mason DE, Peters EC, Urbina HD, Welzel G, Althage A, Liu B, Tuntland T, Jacobson LH, Harris JL, Schumacher AM (2013) Enhanced proteolytic clearance of plasma Aβ by peripherally administered neprilysin does not result in reduced levels of brain Aβ in mice. J Neurosci 33:2457–2464. CrossRef Medline

Wang Q, Zhou Y, Wang X, Evers BM (2006) Glycogen synthase kinase-3 is a negative regulator of extracellular signal-regulated kinase. Oncogene 25:43–50. CrossRef Medline

Wang S, Wang R, Chen L, Bennett DA, Dickson DW, Wang DS (2010) Expression and functional profiling of neprilysin, insulin-degrading enzyme, and endothelin-converting enzyme in prospectively studied elderly and Alzheimer's brain. J Neurochem 115:47–57. CrossRef Medline

Weaver CL, Espinoza M, Kress Y, Davies P (2000) Conformational change as one of the earliest alterations of tau in Alzheimer's disease. Neurobiol Aging 21:719–727. CrossRef Medline

White MF (2006) Regulating insulin signaling and β-cell function through IRS proteins. Can J Physiol Pharmacol 84:725–737. CrossRef Medline

Yan SD, Zhu H, Zhu A, Golabek A, Du H, Roher A, Yu J, Soto C, Schmidt AM, Stern D, Kindy M (2000) Receptor-dependent cell stress and amyloid accumulation in systemic amyloidosis. Nat Med 6:643–651. CrossRef Medline

Yarchoan M, Arnold SE (2014) Repurposing diabetes drugs for brain insulin resistance in Alzheimer disease. Diabetes 63:2253–2261. CrossRef Medline

Yasojima K, Akiyama H, McGeer EG, McGeer PL (2001) Reduced neprilysin in high plaque areas of Alzheimer brain: a possible relationship to deficient degradation of β-amyloid peptide. Neurosci Lett 297:97–100. CrossRef Medline